Research Journal of Applied Sciences, Engineering and Technology 5(4): 1225-1231, 2013
DOI:10.19026/rjaset.5.4854
ISSN: 2040-7459; e-ISSN: 2040-7467

Submitted: June 23, 2012 Accepted: August 17, 2012 Published: February 01, 2013

Research Article

Imaging Simulation of Looking Forward Sonar

Tiedong Zhang, Lei Wan, Shan Ma and Wenjing Zeng
National Key Laboratory of Technology of Autonomous Underwater Vehicles, Department of Shipbuilding Engineering, Harbin Engineering University, Harbin, 150001, P.R. China

Abstract: In this study, we propose a new method for the imaging simulation of looking forward sonar. According to the theory of acoustics, the Kerchief's integral formula is used to solve the scattering sound field of objects in the water and the models of objects are set up. Secondly, the surface of objects is divided into some parts and the formulas are proposed to gain echo data according to the reflecting condition of those parts. These data are used to generate sonar images of objects. At last, the simulation results of echo data and sonar images are contrasted with those gained from the water tank test. The results verified the feasibility of the new method.

Keywords: Echo data, kerchief's integral formula, scattering sound field, sonar image

INTRODUCTION

System simulation technology has become an indispensable tool for the research and development of Autonomous Underwater Vehicle (AUV) (Bharath *et al*., 2006; Folkesson *et al*., 2007; Jian *et al*., 2011). As one of the key technology, the acoustic imaging simulation is paid more attention at present. It not only plays an important role in the closed-loop simulation system, but also its simulation levels are of great significance to improve the whole performance of AUV and deepen the study of underwater perception system (Cufi *et al*., 2002; Horner, 2005; Quidu and Hetet, 2007) .

Simulation of acoustic imaging is in the field of integrated technology, which involves the system simulation technology, acoustic modeling technology and computer technology. Because of the commercial or military reasons, there aren't many published literatures (Mestouri *et al*., 2008). Xu and Feng (2009) used the technology of virtual line in the software of Vega to simulate acoustic image and results were used to carry out the research on the obstacle avoidance and control method of AUV. Didier *et al*. (2007) simulated the acoustic imaging based on the ray theory, parabolic equation and other methods. The simulation framework was found to realize the acoustic imaging simulation under various scenarios. Zhonghua *et al*. (2005) used the functions of collision vector and BUMP features to simulate the performance of some sonars. In short, although some achievements have been made, the research work was mainly focused on the functional simulation of sensor, so the actual situation of acoustic image couldn't be evaluated effectively. It may result in unpredictable problems during real test in the sea.

In this study, in accordance with the acoustics theory, an imaging simulation method of looking forward sonar is proposed. At first, two models of underwater targets are set up and the Kerchief's integral formula is used to solve the scattered sound field of objects in the water and the echo data are generated to form sonar images of objects according to the reflecting condition of acoustic wave in every surface of the object. Simulation results were compared with the experimental data and they show that the method is effective and robust.

DIFFUSE SOUND FIELD OF UNDERWATER OBJECTS

From the acoustics theory, if sound waves encounter obstacles in the way of propagation, secondary sound sources are stirred on the objects surface and they radiate the secondary sound waves to the surrounding medium. These secondary sound waves are usually referred as the scattered waves. Among them, some are reversed back to the sound source and these are known as object echoes. Object echoes are one part of scattering waves and they are generated for the interaction between incident waves and objects. Some features of the target information are also included in the echoes. Therefore, the key problem of sonar sensor simulation is how to identify and solve the scattering sound field of objects in order to generate those echo data (Aimin and Weimin, 2006).

Two ways are usually used. One is to use wave equation to resolve it and the other is to use the Kirchhoff integral method to resolve it. In this study,

Corresponding Author: Tiedong Zhang, National Key Laboratory of Technology of Autonomous Underwater Vehicles, Department of Shipbuilding Engineering, Harbin Engineering University, Harbin, 150001, P.R. China

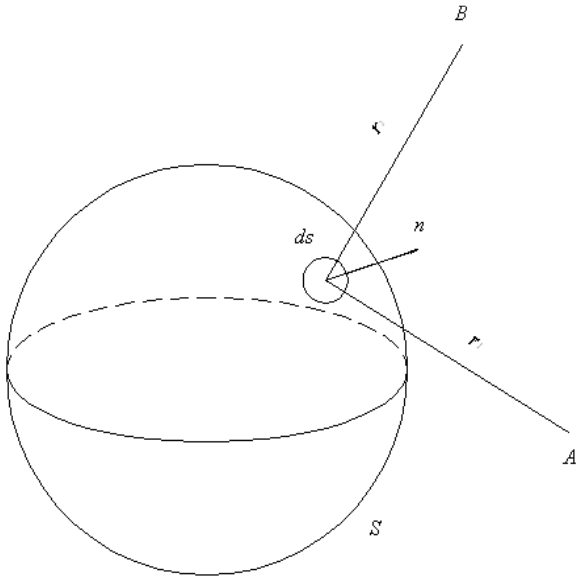

Fig. 1: Geometry relationship of acoustic scattering wave

the last one is selected to analysis the scattering field of two underwater objects. The Kirchhoff integral formula expression is written as:

$$\boldsymbol{\Phi}_2 = \iint_{S_0} (\boldsymbol{\Phi} \frac{\partial \boldsymbol{\Psi}}{\partial n} - \boldsymbol{\Psi} \frac{\partial \boldsymbol{\Phi}}{\partial n}) ds_0 \quad (1)$$

In Eq. (1), S_0 represents the surface areas of scatters and $\boldsymbol{\Phi}(x,y,z) = \boldsymbol{\Phi}_0(x,y,z)e^{-i\omega t}$, where Φ_0 represents the velocity potential on the surfaces of scatters. Ψ Is the auxiliary function and Ψ satisfies the following relationship with Φ:

$$\iiint_v \left(\boldsymbol{\Phi}\nabla^2\boldsymbol{\Psi} - \boldsymbol{\Psi}\nabla^2\boldsymbol{\Phi}\right)dV = \iint_s \left(\boldsymbol{\Phi}\frac{\partial \boldsymbol{\Psi}}{\partial n} - \boldsymbol{\Psi}\frac{\partial \boldsymbol{\Phi}}{\partial n}\right)ds \quad (2)$$

where, $\partial/\partial n$ represents the partial derivative along the outer normal direction of panel ds.

In formula (1), the physical meaning is as following: the situation of secondary radiation on the scatter is decided by sound pressure (velocity potential) in the received point. So if second radiation wave velocity potential φ_s can be gotten at the position where the sonar sensor is placed, based on the acoustic theory, sound pressure $p = \rho\frac{\partial \varphi_s}{\partial t}$ can be defined as $p = \rho\frac{\partial \varphi_s}{\partial t}$ (ρ represents the density of the sound transmission medium).

The sonar sensor simulated in this study is the bilateral high-frequency forward looking sonar. The objects are sphere and cylinder and their shells are composed of the rigid metal material, so the Eq. (1) can be approximated according with the condition of high frequency.

It is supposed that objects are placed in the infinite sound field. The outside surface of object is the closed surface S and the outer normal direction is n, and the sound source point is placed at point A. According to the formula (1), the Kirchhoff integral solution of scattering sound field at point B (Fig. 1) is written as:

$$\boldsymbol{\varphi}_s = -\iint_s \left[\frac{1}{r_2}e^{ikr_2}\cdot\frac{\partial}{\partial \mathrm{n}}(\boldsymbol{\varphi}_s) - \boldsymbol{\varphi}_s\frac{\partial}{\partial \mathrm{n}}\left(\frac{1}{r_2}e^{ikr_2}\right)\right]ds \Big/ 4\pi \quad (3)$$

In formula (3),

k : The wave number

φ_s : The potential function of scattering field

$\partial/\partial n$: The normal derivative on the surface of S. Φ_s

$\frac{\partial}{\partial n}(\boldsymbol{\varphi}_s)$: Unknown values, so the formula (3) can't be resolved directly

According with the boundary condition and far field condition, it can be turned into:

$$\boldsymbol{\varphi}_s = iAk\iint_s \frac{1}{r_1 r_2}e^{ik(r_1+r_2)}\left[\cos(n,r_1) + \cos(n,r_2)\right]ds \Big/ 4\pi \quad (4)$$

Considering the inverse scattering, namely: $r_1 = r_2 = r$ and formula (4) is turned into:

$$\boldsymbol{\varphi}_s = iAk\iint_s \frac{1}{r^2}e^{i2kr}\cos(r,n)ds \Big/ 2\pi \quad (5)$$

So the formula (4) and (5) are the integral solution of scattering field under the condition that the object is rigid.

MODEL OF UNDERWATER OBJECTS

In formula (5), if r and cos(r, n) can be confirmed, φ_s can be gotten. The detail methods are descripted as following:

Model of the rigid sphere: Its radius is R and the distance between the center of the sphere and the sonar is d. The spherical equation is written as $x^2 + y^2 = z^2 = R^2$ and the coordinate system is established (Fig. 2). In the coordinate system, the center of the sphere is at the origin and Z axis is perpendicular to the sonar scanning plane and Y axis is parallel to the scanning centerline of sonar.

The angle between the center line of the sphere in the sonar scanning plane and sonar scanning center line is supposed as α. Point of sight is located at the position of sonar. If connecting line between the sphere center and sonar is on the left of sonar scanning center line,

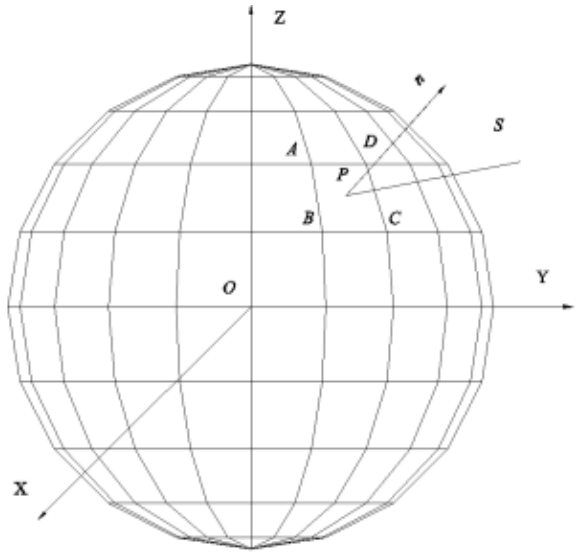

Fig. 2: Scanning situation of rigid sphere

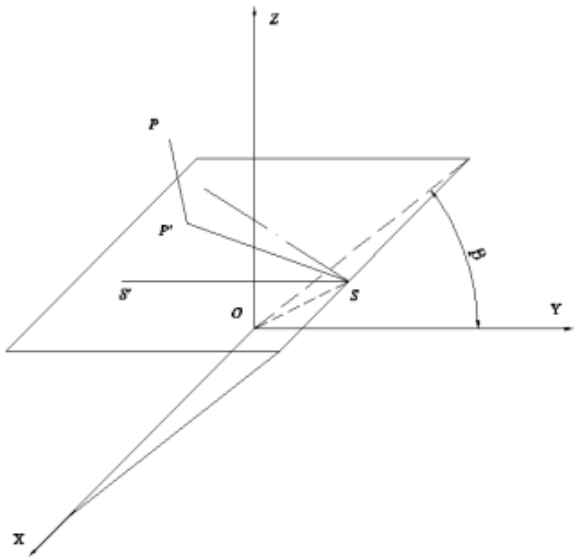

Fig. 3: Determination of scanning angle

the value of α is negative. Otherwise, it is positive. Distance between position of sonar and the origin are d.

The surface of sphere is divided in n equal parts and m equal parts from the forward direction of Z axis and X axis along the radial direction and zonal direction respectively [15], so the values of coordinate at the intersection of each bisector is determined. Supposing that the region ABCD on the surface of sphere is located in the sonar beam and the point A is corresponded to the (i, j) region from the radial and zonal division, so the point A can be written as:

$$A_x = R \times \sin(\pi \times i / n) \times \cos(2\pi / m \times j)$$

$$A_y = R \times \sin(\pi \times i / n) \times \sin(2\pi / m \times j)$$

$$A_z = R \times \cos(\pi / n \times i) \quad (6)$$

Similarly, the point B, C, D and point S(S_x, S_y, S_z) can be obtained. Θ is supposed as the included angle between the projection of connecting line (from point P to point S in the sonar scanning plane) and scanning center line of sonar.

According to the scanned range and scanned step angle of sonar, the echo values produced by the regions can be determined by the following conditions:

i. θ is in the current scan angle scope.
ii. θ is less than half of the vertical detection range.
iii. The distance between two points P and S is in a current scanning step.
iv. The angle, which is between the outside normal vector of point P at the surface of sphere and the vector of point S, is less than 90º.

For the condition (i), θ can be determined as following:

As the axis Z is perpendicular to the sonar scanning plane, the projection point of P is point P', which is represented as (P_x, P_y, P_z) in the plane (Fig. 3), then:

$$\boldsymbol{SP'} = \{P_x - S_x, P_y - S_y, 0\} \quad (7)$$

The sonar scanning center line is represented as SS' and θ between SP' and SS' can be written as:

$$\cos\theta = \frac{\boldsymbol{SP'} \cdot \boldsymbol{SS'}}{|\boldsymbol{SP'}||\boldsymbol{SS'}|} \quad (8)$$

where, θ is determined by the value of P_x and S_x.

Model of the rigid cylinder: Height of cylinder is H and its surface radius is R. The origin of coordinates is set at the bottom center of the cylinder and Z axis is along the height direction. The location of sonar is in the YOZ plane. It is shown in Fig. 4(a).

It is supposed that the angle between the line which connects coordinate origin with sonar and the forward direction of Z axis is set as β. Distance between sonar and origin O is set as d. Intercept in the X axis is set as x, then point S can be obtained as following:

$$S_x = 0$$

$$S_y = d\cos(\frac{\pi}{2} - \beta)$$

$$S_z = d\sin(\frac{\pi}{2} - \beta) \quad (9)$$

The side surface of cylinder is divided into some grids. The numbers of grids are m in radial direction and

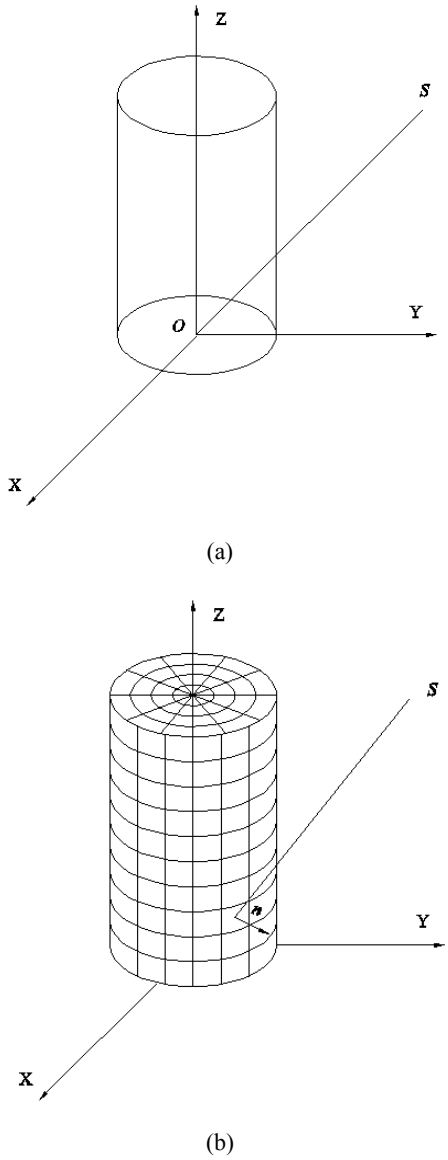

Fig. 4: Coordination and grids (a) cylinder coordinates, (b) results of grids divided on the surface of cylinder

those are n in height direction (as shown in Fig. 4(b). Supposing that the region ABCD on the surface of cylinder is located in the scanning region and the point A is corresponded to the region (i, j), so the point A can be written as:

$$A_x = R\cos(2\pi i/m)$$

$$A_y = R\sin(2\pi i/m)$$

$$A_z = Hj/n \tag{10}$$

Similarly, the point B, C and D can be determined respectively. Considering the geometry relationship among points A, B, C, D, the coordinate values of points P_x, P_y and P_z can be gotten. According to the point P and point S, cos (r, n) can be confirmed.

The end face of cylinder is divided into some grids. The numbers of grids are k in circumferential direction and those are t in radial direction, as shown in Fig. 4(b). Supposing that the region ABCD on the surface of cylinder is located in the sonar beam and the point A is corresponded to the region (i, j), so the coordinate values of point A can be written as:

$$A_x = Rj\cos(2\pi i/k)/t$$

$$A_y = Rj\sin(2\pi i/k)/t$$

$$A_z = 0 \tag{11}$$

Similarly, if point A is on the top surface of the cylinder, then:

$$A_x = Rj\cos(2\pi i/k)/t$$

$$A_y = Rj\sin(2\pi i/k)/t$$

$$A_z = H \tag{12}$$

The condition of echo data produced by the regions is the same as that in sphere. It is as following:

- According to the spatial location of sonar, the surface echo data is determined
- θ is in the current scan angle scope
- θ is less than half of the vertical detection range
- The distance between P and Sis in a current scanning step
- The angle, which is between the outside normal vector of point P at the surface of sphere and the vector of point S, is less than 90°

In the condition (ii), θ can be calculated according to the included angle between two lines and the positive and negative signs of angle can be determined as following:

- When the value of intersection X_0 in X axis is not equal to 0 (Fig. 5), scanning plane center line is intersected the plane XOZ at point Q. P is set as one grid center on the surface of cylinder, which has an effect on the echo at S. P' is the projection point of point in the sonar scan plane. SP' is intersected with plane XOZ at point P_0. Comparing the value of P_0 and Q in X axis, the positive and negative situation of angle between SP' and centerline of sonar scanning plane can be confirmed. If $P_{0x}>Q_x$,

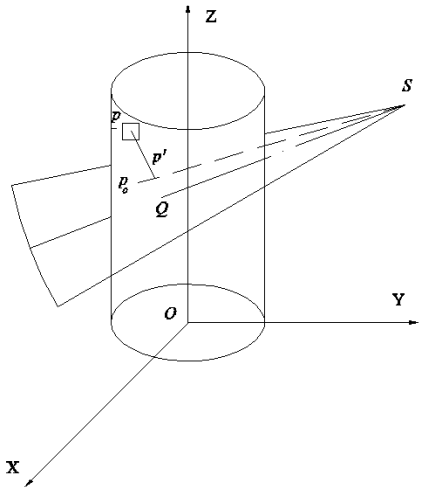

Fig. 5: Confirmation of the sonar scanning angle ($X_0 \neq 0$)

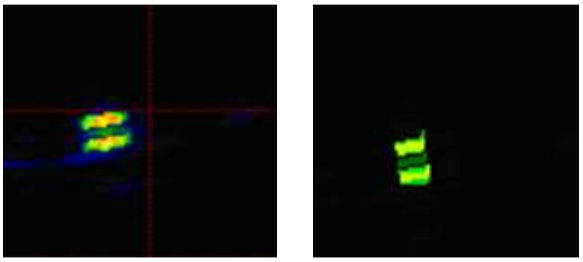

(a) (b)

Fig. 6: Simulation and test results of sphere (a) detected image, (b) simulated image

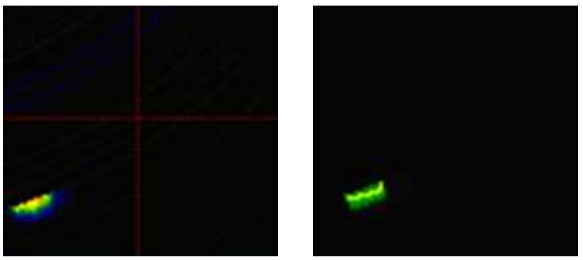

(a) (b)

Fig. 7: Simulation and test results of cylinder (a) detected image, (b) simulated image

the angle is negative value, otherwise, the angle is positive value. By the length of $P'P$ and $P'S$, the angle from PS to sonar scanning plane can be gotten in condition (iii).

- When the value of intersection X_0 in X axis is equal to 0 (Fig. 5), the central axis of cylinder is in the sonar scanning plane. It can be assumed that if the coordinate value of point P' in Z axis is greater than the intersection point between the sonar scanning centerline and Z axis in Z axis, the angle between SP' and sonar scanning plane centerline is positive, otherwise it is negative.

SIMULATION RESULTS AND ANALYSIS

In order to evaluate the imaging simulation results of some single-beam forward looking sonar, some tests of objects detection were carried out. Objects were the hollow aluminum sphere $(r = 0.2m)$ and cylinder $(r = 0.1m, h = 0.3m, l = 0.3m)$. Due to the limit of depth and width of the tank, the measurement range of sonar was less than 5 meters. Simulation and test results were in Fig. 6 to 8.

In Fig. 6a, the sphere was placed at 4.2 m in front of the sonar and the offset angle to the sonar scanning center line was -4.2^0. The corresponding simulation results were shown in Fig. 6b. In Fig. 7a, the cylinder was placed at 4 m in front of the sonar and the angle between the scanning plan and the axis of cylinder was 45^0. The corresponding simulation results were shown in Fig. 7b and results in Fig. 6 and 7 were shown that:

- From the imaging effect, the change of pixel values in the simulation image is not consecutive as in the actual image and they are different in the aspect of the intensity of the noise point and target point. The main reason is that the actual image data displayed is the non-linear processing results of echo data and the data simulated is processed directly by the threshold method. However, for the simulation purposes, the location information of object can be clearly shown in the simulated images, so the requirements of region recognition can be satisfied with.
- From the aspects of target region, no matter the actual images or simulation images, the acoustic imaging outline of the sphere can be shown that it was composed of two parts. It is mainly because the sphere is not rigid entirely. Except that some sound waves are reflected in the form of reflection and scattering waves, another part of the incident waves penetrates the internal objects and stirs the sound field in the object. The inner sound waves is returned to the position of sonar through the reflection and transmission of inner surface. At the same time, under the action of the incident wave, some natural vibration mode of object will be excited, thus some waves are generated with the vibration and these are also received by sonar. So the above-mentioned phenomenon is formed. It can be seen that the simulated image is consistent with the actual situation.

For the forward looking sonar, image data are generated by the sampling transform of sonar data, so the image data is not the real value of echo intensity. It only reflects the strength relationship of echo signal, but for the narrative convenience, it is still referred as "echo intensity".

```
38 31 41 02 01 80 01 09 30 37 2D 4A 55 4C 2D 32 ; 81A..€..07-JUL-2
30 30 33 00 31 36 3A 31 34 3A 32 38 00 2E 31 31 ; 003.16:14:28..11
00 00 00 00 00 4C 00 14 72 00 3C 09 06 04 BA 98 ; .....L..r.<...箙
49 6D 61 67 65 6E 65 78 20 54 65 63 68 6E 6F 6C ; Imagenex Technol
6F 67 79 20 43 6F 72 70 2E 00 00 00 00 00 00 00 ; ogy Corp........
03 E8 00 00 00 00 00 00 00 00 00 00 00 00 00 00 ; .?............
00 00 00 00 49 4D 58 10 40 6F 04 05 00 00 7C 01 ; ....IMX.@o....|.
04 04 03 01 00 00 01 00 00 00 00 00 00 00 00 00 ; ................
00 00 00 00 00 00 00 00 00 00 00 00 00 00 00 00 ; ................
00 00 00 00 00 00 00 00 00 00 00 00 00 00 00 00 ; ................
00 00 00 00 00 00 00 00 00 00 00 00 00 00 00 00 ; ................
00 00 00 00 00 01 04 07 07 05 01 01 00 01 01 00 ; ................
00 00 00 00 00 00 00 00 00 00 00 00 00 00 00 00 ; ................
00 00 00 00 00 00 00 00 00 00 00 00 00 00 00 00 ; ................
00 00 00 00 00 00 00 00 00 00 00 00 00 00 00 00 ; ................
00 00 00 00 00 01 02 02 01 00 01 01 00 00 01 01 ; ................
00 01 01 01 00 00 00 01 01 01 01 01 01 00 00 00 ; ................
01 02 03 03 02 01 00 00 01 01 01 00 01 01 00 00 ; ................
01 01 01 01 01 00 01 01 01 00 00 00 00 00 00 01 ; ................
01 01 01 01 06 0A 0A 05 04 07 08 06 05 06 03 0A ; ................
11 13 12 0D 05 00 03 06 07 05 02 00 00 00 02 01 ; ................
01 04 04 03 01 01 02 03 03 03 03 03 02 01 00 00 ; ................
01 01 01 00 01 02 02 03 07 0A 01 00 FC 00 00 00 ; ............?..
00 00 00 00 00 00 00 00 00 00 00 00 00 00 03 00 ; ................
```

(a)

```
38 31 41 02 01 80 01 09 30 39 2D 4A 41 4E 2D 32 ; 81A..€..09-JAN-2
30 30 34 00 30 38 3A 32 32 3A 30 34 00 2E 33 35 ; 004.08:22:04..35
00 00 00 00 00 0C 06 3D 00 00 14 C9 20 04 BA 98 ; .......=...?.箙
49 6D 61 67 65 6E 65 78 20 54 65 63 68 6E 6F 6C ; Imagenex Technol
6F 67 79 20 43 6F 72 70 2E 00 00 00 00 00 00 00 ; ogy Corp........
02 A3 00 00 00 00 00 00 00 00 00 00 00 00 00 00 ; .?............
00 00 00 00 49 4D 58 10 40 6F 04 3C 00 00 7C 01 ; ....IMX.@o.<..|.
03 02 02 01 04 06 01 01 07 02 00 00 00 00 00 00 ; ................
01 00 01 01 01 00 01 01 02 08 00 03 00 01 01 01 ; ................
02 01 04 02 01 06 00 03 02 01 01 01 06 03 03 06 ; ................
00 01 03 03 02 02 03 00 05 01 06 02 01 01 01 02 ; ................
01 00 00 02 02 03 00 00 02 00 03 04 02 00 03 01 ; ................
05 03 02 02 00 00 02 03 04 02 04 03 01 01 00 00 ; ................
02 01 01 00 02 02 00 02 02 00 03 00 02 06 00 01 ; ................
01 00 01 04 03 05 02 02 05 01 00 01 02 01 03 05 ; ................
02 02 02 01 02 00 03 04 02 03 04 03 00 06 04 00 ; ................
03 00 00 01 00 02 02 07 02 05 03 02 00 07 02 01 ; ................
01 01 00 02 00 00 00 04 01 00 00 01 01 00 01 06 ; ................
01 02 01 02 04 03 00 03 04 04 01 02 00 04 05 01 ; ................
00 02 01 00 01 00 00 02 00 02 12 2E 2C 28 21 19 ; ............,(!.
0E 03 02 02 01 02 03 00 02 02 00 01 00 01 00 00 ; ................
01 01 02 03 01 00 05 02 00 03 00 00 03 00 02 01 ; ................
03 03 00 01 01 00 01 02 00 04 00 00 FC 00 00 00 ; ............?..
00 00 00 00 00 00 00 00 00 00 00 00 00 00 00 00 ; ................
```

(b)

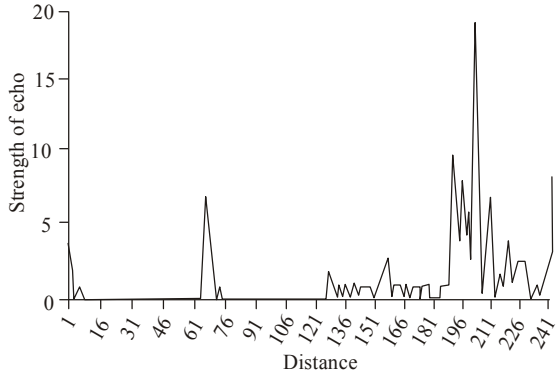

(c)

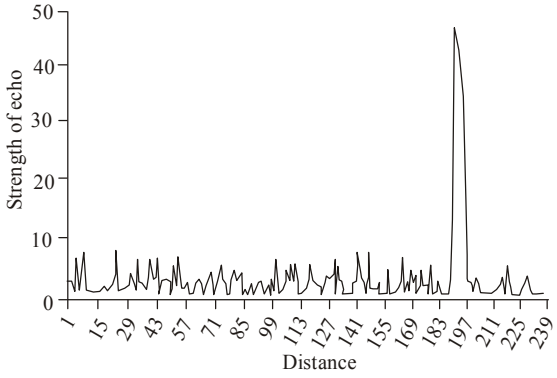

(d)

Fig. 8: Test data and simulation data in the same angle (a) data format gained in the tests, (b) data format gained in the simulation, (c) echo data received in the test, (d) echo data received in the simulation

In Fig. 8a and b, the experimental and simulation data format of sphere is shown. It contains data head (112 characters), echo data (250 characters) and data end (20 characters).In Fig. 8c and d, the curve is generated according with the results in Fig. 8a and b.

Compared the experimental data and simulation data, it can be found that:

- It is difference in the maximum peak value of echo intensity. The reason is mainly that the data conversion in the simulation is not inconsistent with the actual sonar sensor.
- In Fig. 8(d), there is interference of low noise, but it did not appear in Fig. 8(c). In fact, it is consistent with the actual situation of low noise in Fig. 8(d). In Fig. 8(c), due to the impact of noise suppression, the sensor is not sensitive for the low noise, so there is no noise.
- The variable situation of echo signal in the maximum peak position of echo intensity is different. The reason is mainly that the model of sphere in simulation is ideal. But it is corresponding to each other at the maximum peak position. As a whole, the variable trend of echo data in simulation is consistent with that in real situation. Though there are different for the simulation results and test results in the variable trend of noise data and target data, the main purpose of the simulation is to obtain the position information of objects, so the simulation results can meet the requirement of mission.

For the rigid cylinder, the simulation results are similar to those of sphere, so they are not restated here, but two points are emphasized as following:

- In Fig. 7a, the change of sound intensity in the object area is more obvious, but its change is slow in Fig. 7b. It is mainly caused by the difference at the aspect of data processing.
- There is difference for the cylinder and the sphere in the material. It lead that it is difficult for the incident wave to penetrate into the object, so the phenomenon of two acoustic imaging regions to one object does not appear in Fig. 7a, such as in Fig. 6. The results in Fig. 7b also show this situation.

CONCLUSION

The simulation of sonar data is important for the recognition of underwater objects. On the basis of the acoustic theory, a method of sound imaging simulation is proposed. Compared the results of acoustic image and acoustic data, it can draw the following conclusions: selecting the Kirchhoff integral formula to solve underwater scattering field of two typical targets, the echo data can be gotten better and they also reflect the actual detection conditions. The method is accurate and effective.

ACKNOWLEDGMENT

This study is supported in part through grants from National Natural Science Foundation of China (Award: 51009040), the National High Technology Research and Development Program of China (863 Program) (No. 2011AA09A106) and the China Postdoctoral Science Foundation (Award: 2012M510928)

REFERENCES

Aimin, M. and G. Weimin, 2006. Sound reflection and sound shadow simulation technology of high frequency sonar. J. Syst. Simul., 29(6): 2514-2522.

Bharath, K., B. Arjuna and U. Tamaki, 2006. Sonar and vision based navigation schemes for autonomous underwater vehicles. Proceeding of 8th International Conference on Contr. Automat. Robotic. Vision, 1: 437-442.

Cufi, X., R. Garcia and P. Ridao, 2002. An approach to vision-based station keeping for an unmanned underwater vehicle. Proceeding of IEEE/RSJ Interenational Conference on Intelligent Robots and Systems, 1: 799-804.

Didier, G., S. Christophe and G. Rene, 2007. Sonar data simulation based on tube tracing [C]. Proceedings of OCEANS 2007, Europe, pp: 1-6.

Folkesson, J., J. Leonard, J. Leederkerken, 2007. Feature tracking for underwater navigation using sonar. Proceeding of the 2007 IEEE/RSJ International Conference on Intelligent Robots and Systems, San Diego, California, October, 2007, pp: 3678-3684.

Horner, D.P., 2005. AUV experiments in obstacle avoidance. Proceedings of MTS/IEEE, pp: 1464-1470.

Jian, C.A.O., S.U. Yumin and Z. Jinxin, 2011. Design of an adaptive controller for dive-plane control of torpedo-shaped AUV. J. Mar. Sci. Appl., 3(10): 333-340.

Mestouri, H., A. Loussert and G. Keryer, 2008. Simulation of sonar transducer by two-dimensional finite element method. ATILA code and GiD graphical interface. OCEANS 2008 - MTS/IEEE Kobe Techno-Ocean, Numerique, Brest, pp: 1-7.

Quidu, I. and A. Hetet, 2007. AUV (REDERMOR) obstacle detection and avoidance experimental evaluation. Proceedings of OCEANS 2007-Europe, pp: 1-6.

Xu, H.L. and X.S. Feng, 2009. An AUV fuzzy obstacle avoidance method under event feedback supervision. Proceedings of OCEANS 2009, MTS-IEEE Biloxi-Marine Technology for Our Future: Global and Local Challenges. State Key Lab. of Robot, CAS, Shenyang, China, pp: 1-6.

Zhonghua, W., G. Tong and Z. Jimao, 2005. Vega based virtual collision avoiding technology in simulation system of deep-sea ROV's near-ocean-bottom operation. J. Syst. Simul., 17(12): 3089-3090.